Published in final edited form as:
*J Proteome Res*. 2009 March ; 8(3): 1431–1440. doi:10.1021/pr800796j.

# Use of Differential Isotopic Labeling and Mass Spectrometry To Analyze Capacitation-Associated Changes in the Phosphorylation Status of Mouse Sperm Proteins

**Mark D. Platt**[*,†,‡,‖], **Ana M. Salicioni**[§], **Donald F. Hunt**[‖,⊥], and **Pablo E. Visconti**[§]

[†]Department of Chemistry & Chemical Biology, Rensselaer Polytechnic Institute, Troy, New York 12180

[‡]Department of Biology, Rensselaer Polytechnic Institute, Troy, New York 12180

[§]Department of Veterinary and Animal Sciences, University of Massachusetts, Amherst, Massachusetts 01003

[‖]Department of Chemistry, University of Virginia, Charlottesville, Virginia 22908

[⊥]Department of Pathology, University of Virginia, Charlottesville, Virginia 22908

## Abstract

Mammalian sperm need to reside in the female reproductive tract for a finite period of time before acquiring fertilizing competence. The biochemical changes associated with this process are collectively known as “capacitation”. With the use of the mouse as an experimental model, we have previously demonstrated that capacitation is associated with a cAMP-dependent increase in protein tyrosine phosphorylation. However, little is known about the identity and function of the protein targets of this phosphorylation cascade. In the present work, we have used differential isotopic labeling coupled with immobilized metal affinity chromatography (IMAC)-based phosphopeptide enrichment and analysis on a hybrid linear ion trap/FT-ICR mass spectrometer to measure the changes in protein phosphorylation resulting from the capacitation process. As no kinase activators and/or phosphatase inhibitors were used in the preparation of the sperm samples, phosphorylated residues identified in this study represent *in vivo* sites of phosphorylation. Also, in contrast to other methods which rely on the incorporation of isotopically labeled amino acids at the protein level (e.g., SILAC), the present technique is based on the Fisher esterification of protein digests, allowing for the comparison of phosphorylation status in the absence of protein synthesis. This approach resulted in the identification of 55 unique, *in vivo* sites of phosphorylation and permitted the relative extent of phosphorylation, as a consequence of capacitation, to be calculated for 42 different phosphopeptides. This work represents the first effort to determine which specific protein phosphorylation sites change their phosphorylation status *in vivo* as a result of the mammalian capacitation process.

### Keywords

sperm; capacitation; phosphorylation; mouse; mass spectrometry; isotopic labeling



[*]To whom correspondence should be addressed. Mark D. Platt, Department of Chemistry & Chemical Biology, Rensselaer Polytechnic Institute, Troy, NY 12180-3590. Tel: (518) 276-3273. Fax: (518) 276-4887. plattm@rpi.edu.

## Introduction

Mammalian sperm are not able to fertilize an egg immediately after ejaculation. They acquire this ability after residing in the female reproductive tract for a finite period of time. The physiological changes which occur during this period and which make the sperm capable of fertilization constitute the phenomenon of "sperm capacitation".[1,2] With the use of the mouse as an experimental model, we have demonstrated that capacitation is associated with an increase in protein phosphorylation.[3] We have also demonstrated that this increase in phosphorylation, as well as the overall process of capacitation, is regulated by a cAMP-dependent pathway.[4] The presence of this regulatory pathway has since been demonstrated in sperm from other species, including humans.[5,6] Despite these advances in understanding how phosphorylation is controlled during the capacitation process, little is known about the identity of the protein targets of this phosphorylation cascade or of the kinases and phosphatases involved in the regulation of sperm function.

In previous work, two-dimensional polyacrylamide gel electrophoresis (2D-PAGE), anti-phosphotyrosine antibody labeling, and tandem mass spectrometry (MS/MS) were used for the identification of human sperm proteins that specifically undergo tyrosine phosphorylation as a result of the capacitation process.[7] Although this approach was successful in identifying 3 sites of tyrosine phosphorylation on the sperm tail proteins AKAP3 and AKAP4, the sensitivity of the analysis was ultimately limited by the 2D-PAGE separation. Specifically, the losses resulting from additional sample handling and the requirement that proteins be visualized prior to excision prevented the MS/ MS identification of phosphorylation sites on all but the most abundant proteins. In the present work, we circumvented these limitations by avoiding the 2D-PAGE separation altogether, and as we were interested in the global identification of capacitation-induced phosphorylation changes, we avoided the use of antibodies due to the fact that anti-phosphoserine and anti-phosphothreonine antibodies have not yet achieved sufficient selectivity.[8,9]

Although in some cases it is possible to determine the exact site(s) of phosphorylation in a candidate protein using a direct MS/MS shotgun peptide sequencing approach, the phosphorylation site(s) often remain elusive due to the presence of more abundant, nonphosphorylated peptides in the proteolytically digested protein mixture. Previously, iron(III) immobilized metal affinity chromatography (IMAC) was used prior to the MS/MS analysis to enrich for tryptic peptides containing phosphorylated amino acids.[7] In subsequent studies, IMAC selectivity for phosphopeptides was further increased by utilizing the Fisher esterification reaction in which acidic residues are converted to their corresponding methyl esters, thereby preventing the binding of nonphosphorylated peptides to the IMAC resin.[10] In this study, the same approach was used for the global identification of phosphorylation sites, but by carrying out the Fisher esterification with either deuterated or nondeuterated reagent, it also permitted the relative extent of phosphorylation to be calculated for phosphopeptides found in both the capacitated and noncapacitated sperm samples.

Consistent with our previous work,[11] an increase in proline directed serine phosphorylation was observed as a result of the capacitation process for 18 of the phosphopeptides identified in this study. In addition, the tyrosine phosphorylation site for hexokinase I was elucidated, and as predicted,[3,4] the relative extent of phosphorylation at this site did not change as a consequence of capacitation. Interestingly, 3 sites of nonproline directed serine phosphorylation were identified on the sperm tail protein AKAP4 and one of these sites (Ser217) lies within the α-helical region responsible for binding the protein kinase A (PKA) Regulatory II subunit. Taken together, these results confirm the suitability of this approach

for the relative quantitation of capacitation-specific phosphorylation events and provide a basis for subsequent studies designed to elucidate the molecular mechanisms governing this important biological transition.

## Experimental Procedures

### Preparation of Mouse Sperm

Caudal epididymal sperm were collected from CD1 retired breeder males (Charles River Laboratories) sacrificed in accordance with IACUC guidelines. Cauda epididymis from each animal was placed in 1 mL of modified Krebs-Ringer medium (Whitten's-HEPES buffered medium) (WH)[12] containing 100 mM NaCl, 4.7 mM KCl, 1.2 mM $KH_2PO_4$, 1.2 mM $MgSO_4$, 5.5 mM glucose, 1 mM pyruvic acid, 4.8 mM L(+)-lactic acid (hemicalcium salt) in 20 mM HEPES, pH 7.3. This medium, prepared in the absence of bovine serum albumin (BSA) and $NaHCO_3$, does not support capacitation. Sperm released into the media during a 10-min time period were counted and collected by centrifugation at 800*g* for 10 min at room temperature. Sperm pellets were resuspended in either noncapacitating WH medium (without BSA or $NaHCO_3$) or capacitating WH medium (containing 5 mg/mL BSA plus 20 mM $NaHCO_3$) and incubated for 90 min at 37 ° C. In all cases, pH was maintained at 7.3.

### Preparation of Sperm Samples for Mass Spectrometric Analysis

Sperm (approximately $1 \times 10^8$) were incubated in either noncapacitating WH or capacitating WH medium for 90 min at 37 ° C as described above, centrifuged, washed in PBS and then boiled in lysis buffer containing 150 mM NaCl, 0.1% SDS and 25 mM Tris-HCl, pH 7.5, for 5 min. This treatment was sufficient to solubilize cytoskeleton-attached proteins such as AKAP and PERF (data not shown). Proteins solubilized by this method were subsequently treated with trypsin as detailed below.

### Proteolytic Digestion

Aliquots of capacitated and noncapacitated sperm samples containing approximately 800 $\mu$g of total protein in 500 $\mu$L of 0.1 M glacial acetic acid (HOAc) in nanopure water ($nH_2O$) were diluted to 1 mL with 0.1 M ammonium acetate. The samples were digested separately with trypsin at a 1:20 (enzyme/substrate) ratio at 37 °C for 16 h. Each sample was divided into 5 × 200 $\mu$L aliquots (Cap1–5 and NCap1–5) which were then stored at −80 °C.

### Preparation of Peptide Methyl Esters

Four aliquots of each of the frozen samples (Cap1–4 and NCap1–4) were lyophilized completely using vacuum centrifugation. Methanolic 2.25 N HCl (d0 reagent) or DCl (d4 reagent) was prepared by adding 160 $\mu$L of acetyl chloride to 1 mL of anhydrous $d_0$-methyl alcohol or $d_3$-methyl *d*-alcohol dropwise with stirring.[13] After 5 min, 200 $\mu$L of the nondeuterated reagent was added to lyophilized peptide mixtures Cap1, Cap2, NCap1, and NCap2. In the same manner, 200 $\mu$L of the deuterated reagent was added to lyophilized peptide mixtures Cap3, Cap4, NCap3, and NCap4. These solutions were incubated at room temperature for 1 h and dried down completely under vacuum centrifugation, and the procedure was repeated a second time to guarantee full conversion of carboxyl groups to their corresponding methyl esters. The lyophilized, modified sperm protein digests were stored at −80 °C until further use.

### Analysis of Unmodified Digests on the LTQ-FT Mass Spectrometer

Aliquots (20 $\mu$L, ~16 $\mu$g total protein) of each of the unmodified digests (Cap5 and NCap5) were acidified with 0.5 $\mu$L of HOAc and analyzed by nanoflow reversed-phase HPLC (nRPLC) microelectrospray ($\mu$ESI) MS on an LTQ-FT hybrid linear ion trap-Fourier

Transform mass spectrometer. The peptides were loaded, using a pressure bomb, onto a 360 $\mu$m o.d. × 75 $\mu$m i.d. fused-silica precolumn packed with 5 cm of 5–20 $\mu$m C-18 particles behind a LiChrosorb frit. The peptide-loaded precolumn was rinsed to remove salts, re-equilibrated with 0.1% (v/v) HOAc, and connected to a 360 $\mu$m o.d. × 50 $\mu$m i.d. fused-silica in-house fabricated microcapillary analytical column packed with 5 cm of 5 $\mu$m C-18 particles and containing an integrated, micrometer-scale electrospray emitter tip. All column connections were made with 1 cm of Teflon PTFE tubing. Peptides were HPLC gradient eluted into the mass spectrometer (spray voltage = 1.7 kV). Solvent A was 0.1 M HOAc in $nH_2O$ and Solvent B was 0.1 M HOAc in 70% (v/v) acetonitrile (MeCN), 30% (v/v) $nH_2O$. The gradient used was 0–50% B in 50 min, 50–100% B in 10 min, and 100–0% B in 5 min. The instrument was operated in data-dependent mode and cycled through a single MS experiment, using the FT-ICR cell as the detector, and 10 MS/MS experiments, using the linear ion trap, every 3–5 s. All MS/MS scans (collision energy = 35%) were performed with an isolation window of 3 amu (precursor *m/z* ± 1.5 amu). The dynamic exclusion option was selected with a repeat count of 1, a repeat duration of 0.5 min, and exclusion duration of 1 min.

## Immobilized Metal Affinity Chromatography (IMAC)

IMAC was performed as described[14] with modifications. IMAC columns containing 8 cm of POROS MC-20 packing material were rinsed with 1:1:1 methanol (MeOH)/MeCN/0.01% (v/v) HOAc for 5 min at a flow rate of 20 $\mu$L/min. The column was rinsed with $nH_2O$ and metal ions were removed by washing with 50 mM EDTA for 10 min. Excess EDTA was removed by rinsing with $nH_2O$ and the columns were activated with 100 mM $FeCl_3$ at a flow rate of 20 $\mu$L/min for 10 min. Lyophilized, Fisher esterified sperm protein digests were reconstituted in 1:1:1 MeOH/MeCN/0.01% (v/v) HOAc and the IMAC column was rinsed with 20 $\mu$L of the same solution. The peptide solution was then loaded onto the activated IMAC column at a flow rate of 2 $\mu$L/min. The peptide-infused IMAC column was rinsed with 20 $\mu$L of 1:1:1 MeOH/MeCN/0.01% (v/v) HOAc and then connected to a C-18 precolumn, constructed as described above. This entire assembly was re-equilibrated with 5 $\mu$L of 0.1% (v/v) HOAc, after which 100 mM ascorbic acid, introduced at a flow rate of 1 $\mu$L/min for 15 min, was used to reduce the iron(III) and elute the phosphopeptides to the precolumn. Both columns were rinsed for 5 min with 0.1% (v/v) HOAc, the IMAC column was removed, and the precolumn was rinsed independently with 0.1% (v/v) HOAc for 10 min to remove salts before subsequent MS analysis.

## Phosphoproteome Analysis on the LTQ-FT Mass Spectrometer

Differentially labeled aliquots of the same modified sample (i.e., Cap1 ($d_0$ methyl esters) and Cap3 ($d_3$ methyl esters) or NCap1 ($d_0$ methyl esters) and NCap3 ($d_3$ methyl esters)) were combined and subjected to IMAC phosphopeptide enrichment as described above. The phosphopeptide-infused precolumn was connected to an analytical column containing an integrated ESI emitter tip, as described above. Phosphopeptides were HPLC gradient eluted into the mass spectrometer using the dual solvent system described above. However, due to the fact that phosphopeptides often elute from RP packing material at low organic concentration, a shallow gradient of 0–40% B in 90 min, 40–60% B in 10 min, 60–100% B in 10 min, 100% B for 2 min, and 100–0% B in 3 min was used for this analysis.

## Manual Interpretation of Phosphopeptide Spectra

Spreadsheets containing the scan number, precursor mass-to-charge (*m/z*) ratio, charge state, and calculated $[M + H]^+$ value for each MS/MS spectrum were prepared for the two differentially labeled, dissimilar sample analyses (Cap ($d_0$ esters) plus Ncap ($d_3$ esters) and Cap ($d_3$ esters) plus NCap ($d_0$ esters)). Data in each spreadsheet was sorted by precursor *m/z* ratio and potentially associated peptide MS/MS spectra were identified based upon the

expected mass shift (+1.5 amu, +3.0 amu, +4.5 amu, for a +2 peptide ion; +1.0 amu, +2.0 amu, +3.0 amu, for a +3 peptide ion, and so on) and recognition that the deuterium-labeled peptide elutes earlier (within 100 scans) than its hydrogen-labeled counterpart. A similar MS/MS fragmentation pattern, identified by visual inspection, was used to confirm that associated spectra were derived from differentially labeled phosphopeptides with the same primary amino acid sequence. The sequence for each phosphopeptide was determined by *de novo* peptide sequencing: first, the b- and y-ions present in each spectrum were identified and then, beginning from either the N- or C-terminus, the amino acid chain was built sequentially by identifying adjacent b- or y-ion peaks whose mass differences correspond to individual amino acid masses. Sequence assignments were further confirmed by ensuring that the number of carboxylic acids present in the assigned sequence were consistent with the mass shift identified between the calculated $[M + H]^+$ values for the differentially labeled versions of the same peptide (+3 amu for a single carboxylic acid, +6 for two carboxylic acids, etc.). In the case of phosphoserine and phosphothreonine-containing peptides, the neutral loss of phosphoric acid initiated by CAD was also used to confirm the number of phosphate groups in the assigned sequence. In all cases, once a phosphopeptide sequence meeting all criteria was assigned, the second data set was scanned in order to find the same MS/MS spectra for quantitation purposes.

### Global Quantitation of Phosphopeptides from Sperm Total Protein Digests

Differentially labeled aliquots of the dissimilar, esterified samples (i.e., Cap2 ($d_0$ esters) and NCap4 ($d_3$ esters) or NCap2 ($d_0$ esters) and Cap4 ($d_3$ esters)) were combined and subjected to IMAC phosphopeptide enrichment as previously described. The phosphopeptide-infused precolumn was connected to an analytical column containing an integrated ESI emitter tip (1–5 $\mu$m diameter) and peptides were HPLC gradient eluted into the LTQ-FT mass spectrometer as described above. Peptide identifications were made as described under Manual Interpretation of Phosphopeptide Spectra. Quantitation of the relative expression levels of peptides identified in this manner was accomplished by measuring the peak areas corresponding to the identified peptide *m/z* values (±0.02 amu) and the values of their differentially labeled counterparts, where available. The ratio of the capacitated peptide peak area to the noncapacitated peptide peak area was calculated for the peptides in each individual run as a preliminary measurement of the relative quantitation of the two species. The final values for the relative quantitation of each peptide species was calculated by taking the square root of the ratio of the two individual ratios (an odds ratio), which served to compensate for potential systematic errors inherent in comparing the deuterated and the nondeuterated peptides.

## Results

### Comparison of Peptide Levels in Sperm Total Protein Digests

The goal of this research was to analyze changes in phosphorylation that occur as a result of sperm capacitation. For this purpose, cauda epididymal mouse sperm were incubated in conditions that support (+BSA, $+HCO_3^-$) or do not support (−BSA, $-HCO_3^-$) capacitation. A necessary requirement for any attempt at the differential analysis of protein phosphorylation is that identical amounts of protein be compared between dissimilar sample types. To determine if the same amount of protein was present in the capacitated (Cap) and noncapacitated (NCap) aliquots and to confirm that both samples had been subjected to identical digestion conditions, a separate analysis of each of the digests (not subjected to Fisher esterification (Cap5 and NCap5)) was conducted on the LTQ-FT mass spectrometer. The peak areas corresponding to a tryptic peptide from a nuclear protein constitutively expressed in mouse testis (RDGFVTSKRKK; *m/z* = 441.28) and a peptide resulting from the autodigestion of trypsin (VATVSLPR; *m/z* = 421.76) were compared and found to have a

ratio of 0.92 and 1.26, respectively (Figure 1) demonstrating similar protein levels and extent of digestion.

### Intrasample Comparison of Phosphopeptide Levels in Protein Digests

The selective IMAC enrichment of phosphorylated peptides from the highly complex capacitated and noncapacitated solution digests was expected to be problematic due to the fact that acidic residues (i.e., glutamic and aspartic acid) have been shown to bind to immobilized iron atoms.[15] To prevent nonphosphorylated, acidic residue-containing peptides from interfering with the analysis, peptide carboxylic acids in each sample were converted to their corresponding methyl esters using either unlabeled or deuterium-labeled methanol as a reagent in two separate sets of reactions. While this was crucial for the subsequent quantification of differential phosphopeptide expression in each sample, these separate reactions added another variable that had to be considered before a differential analysis could be conducted. To determine if each reaction had proceeded to the same extent, Fisher esterification on equal amounts of each sample was conducted using both $d_0$- and $d_4$-reagent. The differentially modified peptides from the same sample types, either capacitated or noncapacitated (NCap ($d_0$ esters) and NCap ($d_3$ esters) or Cap ($d_0$ esters) and Cap ($d_3$ esters)), were then combined and analyzed using the IMAC-nRPLC-MS/MS analysis described above. The peak areas corresponding to a tryptic phosphopeptide from the calcium binding tyrosine phosphorylation regulated protein (CABYR) (TKIpSIepSLK; $m/z$ = 603.79 ($d_0$ labeled) and 606.81 ($d_3$ labeled)) were compared in both sample types and found at a ratio of 0.99 in the noncapacitated samples and at 0.95 in the capacitated samples (Figure 2). These results confirmed that the differential labeling proceeded to the same extent in each modification reaction. Importantly, these experiments also served as controls for the subsequent experiments in which differentially labeled, dissimilar sample types (NCap ($d_0$ esters) versus Cap ($d_3$ esters) or NCap ($d_3$ esters) versus Cap ($d_0$ esters)) were compared.

### Value of Differential Isotopic Labeling for Phosphopeptide Identification

The assignment of peptide sequences to phosphopeptide spectra is often hindered by the fact that phosphoserine and phosphothreonine residues demonstrate the neutral loss of phosphoric acid, not only from the intact peptide, but also from phosphate-containing fragments generated during CAD, the process whereby peptides are fragmented along the backbone as a result of collisions with an inert bath gas inside the ion trap.[16] This results in a crowded MS/MS spectrum dominated by peaks that do not correspond to sequence-informative ions and which result in spurious peptide sequence assignments. A convenient consequence of the Fisher esterification protocol followed in this study is that comparison of the MS and MS/MS data acquired for the identical, but differentially labeled phosphopeptides, is of remarkable utility in assigning their proper sequences. First, a visual inspection of the isotopic patterns from each phosphopeptide reveals their charge state and, by comparing the mass shift between the two different isotopic envelopes, allows for the determination of the number of acidic residues in the peptide. For example, as shown in Figure 3, the difference of 0.5 amu between the $^{12}C$ and $^{13}C$ isotopes for $m/z$ = 603.79 and $m/z$ = 606.81 indicates that these peptides both have a charge of +2. In addition, the mass shift of 3.02 amu between $m/z$ = 603.79 and $m/z$ = 606.81 reveals that this peptide contains 2 modifications, one at the C-terminus (always present) and one on either a glutamic or aspartic acid residue. Both observations agree with the assigned sequence of TKIpSIepSLK, which can be further confirmed by comparison of the MS/MS spectra from each peptide. As Figure 4 demonstrates, b- and y-type ions are easily picked out of each spectrum based upon their respective mass shifts: y-ions will always be shifted by at least 3 amu in the deuterium labeled peptide due to the presence of the carboxy-terminus, while b-ions will only reveal a shift once they contain a modified acidic residue. The information gained in this manner by

FT-ICR analysis (accurate mass and number of carboxyl groups) can be coupled with the complementary information provided by the MS/MS analyses (fragment ions, sequence tags, and minimum number of phosphorylated residues from neutral losses of phosphoric acid) to rapidly identify the correct peptide sequence.

## Identification of Phosphopeptides from Sperm Total Protein Digests

Once each sample type was determined to contain the same amount of protein, and that the alternative labeling experiments had not disturbed this ratio, a differential analysis of phosphopeptide expression, using two similar, but not identical, experiments was conducted. In the first experiment, the heavy isotope-labeled capacitated protein digest was combined with the light isotope-labeled noncapacitated digest (Cap ($d_3$ esters) vs NCap ($d_0$ esters)), while in the second experiment, the $d_3$ modified noncapacitated sample was combined with the $d_0$ modified capacitated sample (Cap ($d_0$ esters) vs NCap ($d_3$ esters)). These combined samples were then subjected to IMAC for phosphopeptide enrichment and independently analyzed on the LTQ-FT hybrid linear ion trap-Fourier Transform mass spectrometer. While the total ion chromatograms (TIC) for each analysis were remarkably similar, as expected, the relative intensities of pairs of peaks were reversed between analyses (Figure 5). Visual comparison of the MS spectra acquired during each chromatographic gradient identified hundreds of phosphopeptide pairs, but software designed to analyze these pairs and identify differences automatically has not yet been completed. Instead, all MS/MS spectra were confirmed by manual interpretation of the corresponding MS/MS sequence(s). Importantly, every carboxylic acid-containing residue in every identified phosphopeptide had been modified, suggesting that our derivatization method proceeded to completion, effectively preventing the binding of carboxylic acid-containing peptides to the IMAC column.

## Intersample Comparison of Phosphopeptide Levels in Protein Digests

Peak ratios of the corresponding deuterated and nondeuterated phosphopeptides were used to derive relative levels of each peptide in the respective samples. As we were primarily interested in the level of the phosphopeptides identified in the capacitated sample relative to the phosphopeptides identified in the noncapacitated samples, the capacitated peak area was divided by the noncapacitated peak area for each peptide in each analysis (Figure 6). The design of the overall experimental scheme (Cap ($d_0$ esters) vs NCap ($d_3$ esters) and Cap ($d_3$ esters) vs NCap ($d_0$ esters)) also permitted the calculation of the square of the odds ratio, or ratio of ratios, for each peptide pair, which compensated for differences in the creation or detection of $d_0$ labeled peptides in relation to $d_3$ labeled peptides. With the use of this technique, the relative abundances of 42 of the 44 phosphopeptides identified above were determined and represented a range of values (Table 1). While several of these peptides do not appear to vary significantly, others were found to have an increased representation in the capacitated sample, strongly suggesting the phosphorylation of these sequences as a result of the capacitation process. For example, the phosphopeptide LIpSSeNFeNYVR from fatty acid binding protein 9, also known as PERF15,[17] was only detected in the capacitated sample. Contrary to the increased representation observed in some cases, other phosphopeptides were found to be more abundant in the noncapacitated sample, suggesting that these sequences undergo dephosphorylation during sperm capacitation. One example of this is the phosphorylated peptide AIVpSPPVeMVeeIpSK which was determined to be highly upregulated in the noncapacitated sample. Our data also indicate that several peptides undergo proline-directed phosphorylation; this finding is in agreement with previous results from our laboratory demonstrating that proline-directed phosphorylation is upregulated in mouse sperm as a result of the capacitation process.[11] In addition, hexokinase, a highly abundant sperm protein which has been shown to be tyrosine-phosphorylated to the same extent in both noncapacitated and capacitated mouse sperm using alternative biochemical techniques,[3,18] was shown to be phosphorylated at Tyr31 in this study and the relative extent

of phosphorylation at this site between capacitated and noncapacitated sperm was determined to be 1.15. This observation further confirms the usefulness of differential isotopic labeling for the relative quantitation of phosphorylation in a cell exposed to a particular stimulus.

## Discussion

Mammalian sperm are not capable of fertilization immediately after ejaculation. In 1951, Chang[1] and Austin[2] independently demonstrated that mammalian sperm require residence in the female tract for a period of time to acquire their fertilizing capacity. Following these original observations, many studies confirmed that the environment of the female tract induces a series of physiological changes in the sperm; these changes are collectively called “capacitation”. This maturational process is associated with the activation of a phosphorylation cascade in which protein kinase A (PKA), a serine/ threonine kinase, is upstream of the increase in tyrosine phosphorylation of several proteins.[19] To understand, at the molecular level, the function of this phosphorylation cascade, as well as how it is regulated, it is important to identify the proteins that change their phosphorylation status during capacitation. Recently, identification of proteins that become tyrosine phosphorylated during this process has been conducted using a combination of 2D-PAGE and MS/MS.[7,20] However, very little is known about proteins phosphorylated during capacitation on serine or threonine residues. In the present manuscript, a global approach has been taken to compare the phosphorylation status of sperm incubated in conditions that either support or do not support capacitation. Importantly, this study was designed to identify *in vivo* sites of phosphorylation rather than using cells treated with kinase activators/phosphatase inhibitors or cells genetically modified to overexpress specific proteins.

Phosphorylation by protein kinases forms the basis of intracellular signaling networks, including transduction of extracellular signals, intracellular transport, and cell cycle progression. Among the many methods used to study protein phosphorylation, mass spectrometric identification of phosphorylation sites is preferred due to its speed and high sensitivity.[21] Although methods have been developed to isolate phosphopeptides in the mass spectrometer on the basis of CAD-induced neutral losses,[22] competitive ionization with nonphosphorylated peptides in the source limits the overall suitability of this method for the global identification of phosphorylation sites from complex mixtures. Instead, a majority of current methods utilize a phosphopeptide enrichment step prior to mass spectrometric analysis.[23-25] In a recent study, over 2200 nonredundant phosphorylation sites were identified in *Saccharomyces cerevisiae* following iron(III) IMAC-based phosphopeptide enrichment and analysis on an LTQ-Orbitrap mass spectrometer.[26] Although a similar enrichment methodology was employed here, the ultimate goal of this study was not only to identify the specific sites of phosphorylation present in a capacitated sperm population, but also to compare the relative extent of phosphorylation occurring at these sites as a result of the capacitation process.

Similar to other high-throughput methodologies such as microarrays, the advantage of a global phosphoproteomics approach is that this method is unbiased and capable of generating an extensive amount of data in a relatively short time. However, more targeted information can be achieved when this technique is used to analyze the functional changes occurring in a biological process. Because different peptides have different ionization efficiencies and mass spectrometric responses, mass spectrometry is not amenable for direct quantification. However, stable-isotope analogues of a chemical entity can be compared and used for relative quantification between two or more differentially labeled populations. In proteomics, differential isotopic labeling can be achieved by chemical modification[27] or by metabolic labeling.[28] In the present work, the esterification of peptide carboxylic acids was

used primarily to prevent nonphosphorylated peptides in the complex mixture from interfering with the IMAC-based phosphopeptide enrichment. However, by taking advantage of this chemical modification and conducting the Fisher esterification with both deuterated and nondeuterated methanol, it became possible to quantify phosphopeptide expression between the capacitated and noncapacitated samples. Signals for phosphopeptides present in both samples appeared as doublets in the MS spectra separated by $n$(3 Da)/$z$ (where $n$ is the number of carboxylic acid groups n the peptide and $z$ is the charge on the peptide). The ratio of the two signals changes as a function of the phosphorylation or dephosphorylation that occurs during the capacitation process. At the same time, peptides were isolated and fragmented using CAD in the linear ion trap to provide MS/MS spectra for subsequent phosphopeptide sequencing. This methodology allowed for the determination of capacitation-dependent changes in phosphorylation; moreover, comparison of doublets gave a quantitative estimate of the level of phosphorylation of each sequence and the ability to analyze exact phosphorylation sites. Interestingly, a phosphotyrosine containing peptide from hexokinase type I was identified and determined to be present at the same level in both sample types. This finding is consistent with previous reports[3] indicating that hexokinase type I is tyrosine phosphorylated in mouse sperm.

A fortunate consequence of this approach was that the differential labeling procedure also aided in the sequencing of the phosphopeptide spectra. The fact that deuterated and nondeuterated forms of the same peptide nearly coelute (deuterated forms having a slightly lower retention time) coupled with the accurate mass measurements from the high resolution FT-ICR mass spectra allows for quick correlation of related peptide species. The use of this information in combination with the readily discernible peptide charge state allows for the number of modifications to be determined in each phosphopeptide. The knowledge of the number of acidic residues in a given peptide greatly limits the number of potentially “correct” peptide assignments and manual inspection of the deuterated and nondeuterated MS/MS spectra quickly reveals the types of ions present (b- or y-type ions), permitting further refinement. As this study required a comprehensive analysis of peptide expression in a complex mixture, all analyses were conducted on LTQ-FT hybrid linear ion trap-Fourier Transform mass spectrometer, a technology particularly well-suited to the analysis of differential peptide/protein expression.

Among the sites presenting a capacitation-associated increase in phosphorylation was the phosphopeptide LIpSSeNFeNYVR, from fatty acid binding protein 9, also known as PERF15.[29,30] PERF15 is a testis-specific protein and it is the major protein component of the sperm structure known as perforatorium in the perinuclear theca, which is found between the inner acrosomal and the outer face of the nuclear envelope of the sperm head. Our results demonstrate a capacitation-dependent phosphorylation of PERF15 on the Ser3 residue. In the context of our findings, it has been shown that another fatty acid binding protein family member, the 422 protein, is also regulated by phosphorylation.[31] It is tempting to speculate that similar changes in phosphorylation, occurring as a result of capacitation, may be functionally relevant for PERF15.

In the highly polarized sperm cell, various compartmentalized functions are regulated by protein kinase A (PKA) signaling. In particular, sperm capacitation has been associated with the activation of a phosphorylation cascade in which PKA, a serine/ threonine kinase, is upstream of the increase in tyrosine phosphorylation of several proteins.[19] Taking this into account, the finding that several sites belonging to the sperm-specific A-kinase anchor protein 4 (AKAP4) are phosphorylated during capacitation is noteworthy. In particular, we note that the peptide LSpSLVIQMAR increased its phosphorylation by a factor of 4.62 in the capacitated sample. This peptide is part of the α helix involved in the binding of AKAP4

to PRKAR2 (RIIα)[32,33] and changes in the charge density of this α helix due to phosphorylation may have consequences in the binding of AKAP4 to RII and therefore affect cAMP-dependent signaling.

Almost half of the peptides found to be phosphorylated as a result of capacitation corresponded to proline-directed phosphorylation sites. These observations are in agreement with previous work from our laboratory[11] and from others.[34] Among proline-directed kinases, ERK1/2 are present in mouse sperm; however, two different ERK pathway inhibitors, U0126 and PD098059, were not able to block the capacitation-associated increase in proline-directed phosphorylation.[11] Further studies will be necessary to determine the role of this kinase, other proline-directed kinases, and the overall relevance of proline-directed phosphorylation in mouse sperm capacitation. Although our analysis has been limited to date, these results are encouraging and it is believed that more phosphorylation sites will be identified in the future, as a comparison of the high-resolution MS spectra identified several differentially labeled peak pairs. Toward this goal, development of software to simplify the analysis is currently ongoing and the use of electron transfer dissociation (ETD) as an alternative to CAD for phosphopeptide fragmentation is being explored. The methodology presented here goes beyond the field of reproductive biology and could be used to understand signaling mechanisms in a wide array of biological systems.

## Acknowledgments

This study was supported by NIH HD38082 and NIH HD44044 grants (to P.E.V.) and GM 37537 grant (to D.F.H.).

## References

1. Chang MC. Fertilizing capacity of spermatozoa deposited into the fallopian tubes. Nature 1951;168:697–698. [PubMed: 14882325]
2. Austin CR. Observations on the penetration of the sperm in the mammalian egg. Aust J Sci Res Ser B 1951;4:581–596. [PubMed: 14895481]
3. Visconti PE, Bailey JL, Moore GD, Pan D, Olds-Clarke P, Kopf GS. Capacitation of mouse spermatozoa. I. Correlation between the capacitation state and protein tyrosine phosphorylation. Development 1995;121:1129–1137. [PubMed: 7743926]
4. Visconti PE, Moore GD, Bailey JL, Leclerc P, Connors SA, Pan D, Olds-Clarke P, Kopf GS. Capacitation of mouse spermatozoa. II. Protein tyrosine phosphorylation and capacitation are regulated by a cAMP-dependent pathway. Development 1995;121:1139–1150. [PubMed: 7538069]
5. Leclerc P, de Lamirande E, Gagnon C. Cyclic adenosine 3′,5′ monophosphate-dependent regulation of protein tyrosine phosphorylation in relation to human sperm capacitation and motility. Biol Reprod 1996;55:684–692. [PubMed: 8862788]
6. Osheroff JE, Visconti PE, Valenzuela JP, Travis AJ, Alvarez J, Kopf GS. Regulation of human sperm capacitation by a cholesterol efflux- stimulated signal transduction pathway leading to protein kinase A- mediated up-regulation of protein tyrosine phosphorylation. Mol Hum Reprod 1999;5:1017–1026. [PubMed: 10541563]
7. Ficarro S, Chertihin O, Westbrook VA, White F, Jayes F, Kalab P, Marto JA, Shabanowitz J, Herr JC, Hunt D, Visconti PE. Phosphoproteome analysis of human sperm. Evidence of tyrosine phosphorylation of AKAP 3 and valosin containing protein/P97 during capacitation. J Biol Chem 2003;278:11579–11589. [PubMed: 12509440]
8. Johnson SA, Hunter T. Kinomics: methods for deciphering the kinome. Nat Methods 2005;2:17–25. [PubMed: 15789031]
9. Reinders J, Sickmann A. State-of-the-art in phosphoproteomics. Proteomics. Proteomics 2005;5:4052–4061. [PubMed: 16196093]
10. Ficarro SB, McCleland ML, Stukenberg PT, Burke DJ, Ross MM, Shabanowitz J, Hunt DF, White FM. Phosphoproteome analysis by mass spectrometry and its application to Saccharomyces cerevisiae. Nat Biotechnol 2002;20:301–306. [PubMed: 11875433]

11. Jha KN, Salicioni AM, Arcelay E, Chertihin O, Kumari S, Herr JC, Visconti PE. Evidence for the involvement of proline-directed serine/threonine phosphorylation in sperm capacitation. Mol Hum Reprod 2006;12:781–789. [PubMed: 17050774]
12. Moore GD, Ayabe T, Visconti PE, Schultz RM, Kopf GS. Roles of heterotrimeric and monomeric G proteins in sperm-induced activation of mouse eggs. Development 1994;120:3313–3323. [PubMed: 7720569]
13. Knapp DR. Chemical derivatization for mass spectrometry. Methods Enzymol 1990;193:314–329. [PubMed: 2074824]
14. Lin C, Platt M, Ficarro S, Hoofnagle M, Shabanowitz J, Comai L, Hunt D, Owens G. Mass spectrometric identification of phosphorylation sites of rRNA transcription factor upstream binding factor. Am J Physiol Cell Physiol 2007;292(5):C1617–1624. [PubMed: 17182730]
15. Posewitz MC, Tempst P. Immobilized gallium(III) affinity chromatography of phosphopeptides. Anal Chem 1999;71:2883–2892. [PubMed: 10424175]
16. DeGnore JP, Quin J. Fragmentation of phosphopeptides in an ion trap mass spectrometer. J Am Soc Mass Spectrom 1998;9:1175–1188. [PubMed: 9794085]
17. Pouresmaeili F, Morales CR, Oko R. Molecular cloning and structural analysis of the gene encoding PERF 15 protein present in the perinuclear theca of the rat spermatozoa. Biol Reprod 1997;57:655–659. [PubMed: 9283004]
18. Kalab P, Visconti P, Leclerc P, Kopf GS. p95, the major phosphotyrosine-containing protein in mouse spermatozoa, is a hexokinase with unique properties. J Biol Chem 1994;269:3810–3817. [PubMed: 7508920]
19. Visconti PE, Westbrook VA, Chertihin O, Demarco I, Sleight S, Diekman AB. Novel signaling pathways involved in sperm acquisition of fertilizing capacity. J Reprod Immunol 2002;53:133–150. [PubMed: 11730911]
20. Bailey JL, Tardif S, Dube C, Beaulieu M, Reyes-Moreno C, Lefievre L, Leclerc P. Use of phosphoproteomics to study tyrosine kinase activity in capacitating boar sperm Kinase activity and capacitation. Theriogenology 2005;63:599–614. [PubMed: 15626419]
21. Bakalarski C, Haas W, Dephoure N, Gygi S. The effects of mass accuracy, data acquisition speed, and search algorithm choice on peptide identification rates in phosphoproteomics. Anal Bioanal Chem 2007;389(5):1409–1419. [PubMed: 17874083]
22. Edelson-Averbukh M, Pipkorn R, Lehmann W. Phosphate group-driven fragmentation of multiply charged phosphopeptide anions. Improved recognition of peptides phosphorylated at serine, threonine, or tyrosine by negative ion electrospray tandem mass spectrometry. Anal Chem 2006;78(4):1249–1256. [PubMed: 16478119]
23. Oda Y, Nagasu T, Chait BT. Enrichment analysis of phosphorylated proteins as a tool for probing the phosphoproteome. Nat Biotechnol 2001;19:379–382. [PubMed: 11283599]
24. Pinkse M, Uitto P, Hilhorst M, Ooms B, Heck A. Selective isolation at the femtomole level of phosphopeptides from proteolytic digests using 2D-NanoLC-ESI-MS/MS and titanium oxide precolumns. Anal Chem 2004;76(14):3935–3943. [PubMed: 15253627]
25. Ficarro S, Parikh J, Blank N, Marto J. Niobium(V) oxide (Nb2O5): application to phosphoproteomics. Anal Chem 2008;80(12):4606–4613. [PubMed: 18491922]
26. Li X, Gerber S, Rudner A, Beausoleil S, Haas W, Vill©n J, Elias J, Gygi S. Large-scale phosphorylation analysis of alpha-factor-arrested *Saccharomyces cerevisiae*. J Proteome Res 2007;6(3):1190–1197. [PubMed: 17330950]
27. Shiio Y, Aebersold R. Quantitative proteome analysis using isotope-coded affinity tags and mass spectrometry. Nat Protoc 2006;1(1):139–145. [PubMed: 17406225]
28. Mann M. Functional and quantitative proteomics using SILAC. Nat Rev Mol Cell Biol 2006;7:952–958. [PubMed: 17139335]
29. Oko R, Morales CR. A novel testicular protein, with sequence similarities to a family of lipid binding proteins, is a major component of the rat sperm perinuclear theca. Dev Biol 1994;166:235–245. [PubMed: 7958448]
30. Korley R, Pouresmaeili F, Oko R. Analysis of the protein composition of the mouse sperm perinuclear theca and characterization of its major protein constituent. Biol Reprod 1997;57:1426–1432. [PubMed: 9408250]

31. Hresko RC, Hoffman RD, Flores-Riveros JR, Lane MD. Insulin receptor tyrosine kinase-catalyzed phosphorylation of 422(aP2) protein. Substrate activation by long-chain fatty acid. J Biol Chem 1990;265:21075–21085. [PubMed: 2174434]

32. Visconti PE, Johnson LR, Oyaski M, Fornes M, Moss SB, Gerton GL, Kopf GS. Regulation, localization, and anchoring of protein kinase A subunits during mouse sperm capacitation. Dev Biol 1997;192:351–363. [PubMed: 9441673]

33. Miki K, Eddy EM. Identification of tethering domains for protein kinase A type Ialpha regulatory subunits on sperm fibrous sheath protein FSC1. J Biol Chem 1998;273:34384–34390. [PubMed: 9852104]

34. de Lamirande E, Gagnon C. The extracellular signal-regulated kinase (ERK) pathway is involved in human sperm function and modulated by the superoxide anion. Mol Hum Reprod 2002;8:124–135. [PubMed: 11818515]

## Abbreviations

| | |
|---|---|
| PBS | phosphate-buffered saline |
| WH | Whitten's-HEPES buffered medium |
| BSA | bovine serum albumin |
| $HCO3^-$ | bicarbonate ion |
| dbcAMP | dibutyryladenosine 3′5′-cyclic monophosphate |
| PKA | protein kinase A |
| 2D-PAGE | two-dimensional polyacrylamide gel elechtrophoresis |
| IMAC | immobilized metal affinity chromatography |
| $\mu$ESI | microelectrospray ionization |
| CAD | collisionally activated dissociation |
| MS/MS | tandem mass spectrometry |
| HOAc | glacial acetic acid |
| HPLC | high-performance liquid chromatography |
| nRPLC | nanoflow reversed-phase HPLC |
| LTQ-FT | linear ion trap-Fourier Transform |
| MeCN | acetonitrile |
| MeOH | methanol |
| K-OMe | Fisher esterified C-terminal lysine |
| FT-ICR | Fourier Transform ion cyclotron resonance |
| TIC | total ions chromatograms |

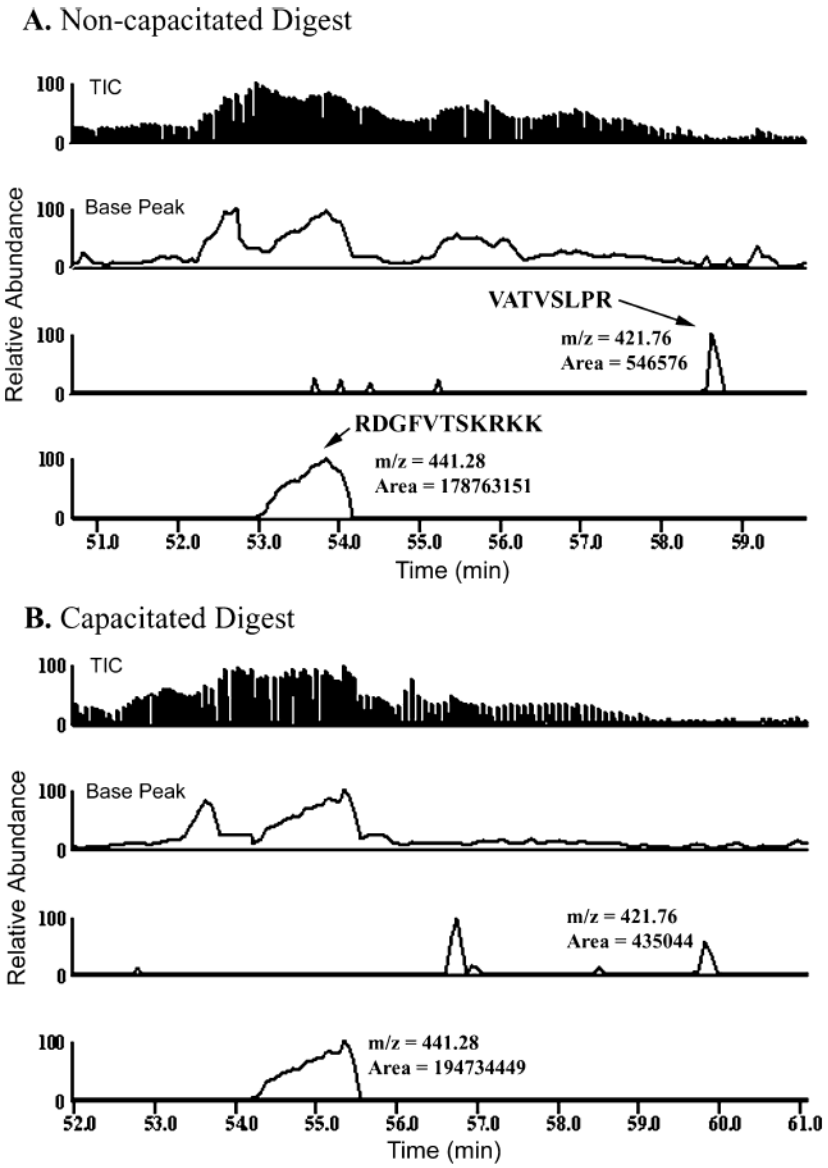


**Figure 1.**

Comparison of peptides identified in noncapacitated (A) and capacitated (B) sperm total protein digests. The peak at *m/z* = 421.76 was identified through MS/MS analysis to be the tryptic peptide VATVSLPR from the autodigestion of trypsin, while the peak at *m/z* = 441.28 was identified through MS/MS analysis to be the tryptic peptide RDGFVTSKRKK from a sperm nuclear protein. The ratio of the peak areas between the noncapacitated and capacitated digests is 1.26 and 0.92, respectively.

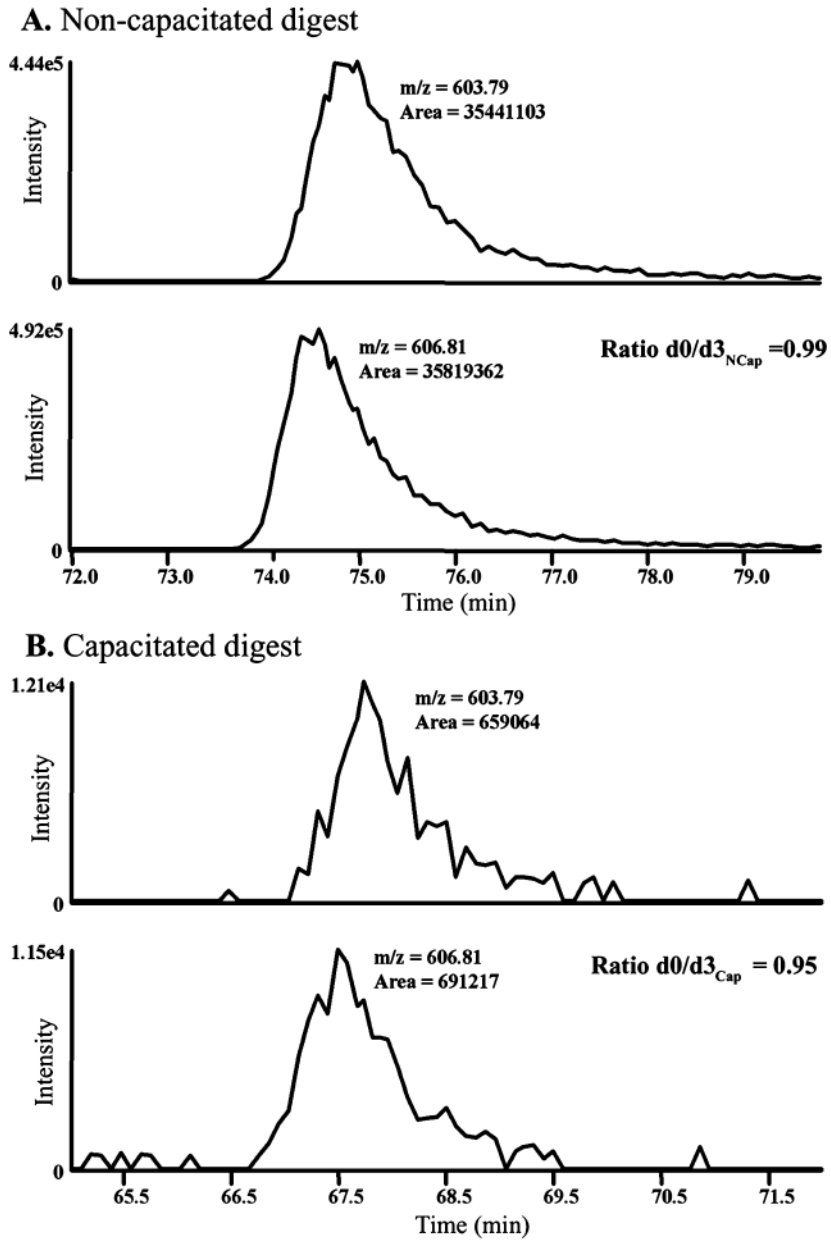


**Figure 2.**

Intrasample comparison of noncapacitated and capacitated digests. Comparison of differentially labeled phosphopeptide peak areas identified in an IMAC analysis of a combination of equal amounts of CH3 and CD3 Fisher esterified noncapacitated (A) and capacitated (B) sperm total protein digests. The $d_0/d_3$ peak ratio was 0.99 in the noncapacitated sample and 0.95 in the capacitated sample, confirming equal amounts of this peptide in the CH3 and CD3 Fisher esterified samples from similar capacitation states.

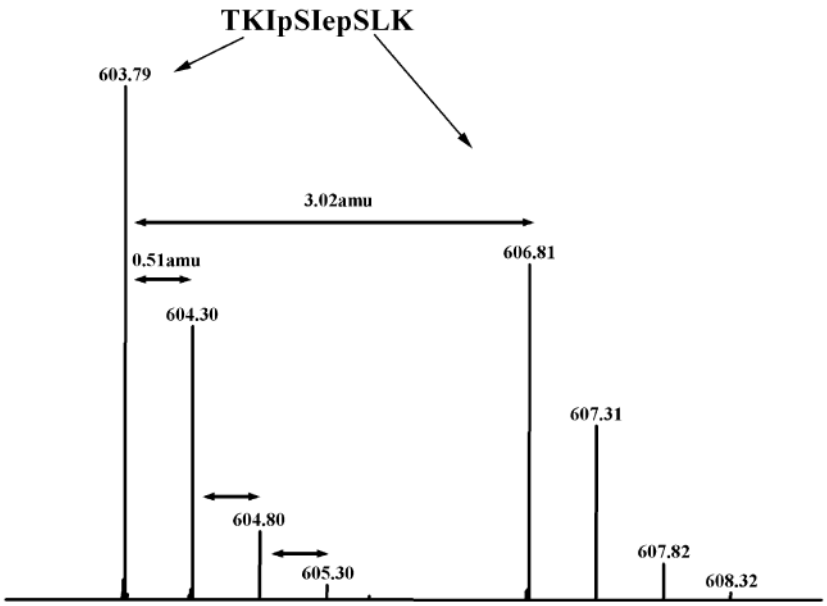


$$\frac{\text{(Charge state) x (Mass difference)}}{3} = \text{number of modifications}$$

$$\frac{(2) \text{ x } (3)}{3} = 2 \text{ modifications}$$

**Figure 3.**

Isotopic distributions of the doubly charged deuterated and nondeuterated TKIpSIepSLK peptides from a single scan, where both peptides were eluting from the HPLC column. The accurate mass measurements (5 ppm in this case) provided by using the FT-ICR cell as the detector on the LTQ-FT instrument revealed these peptides to be doubly charged (mass difference of 0.5 amu within individual isotopic envelopes) and related (mass difference of 3.020 amu between isotopic envelopes). The number of carboxyl groups contained in the peptides was determined using the equation indicated in Figure 3. Mass difference refers to the difference between the monoisotopic masses of related deuterated and nondeuterated peptides, and charge state refers to the reciprocal of the mass difference between $^{12}C$ and $^{13}C$ peaks in the same charge envelope.

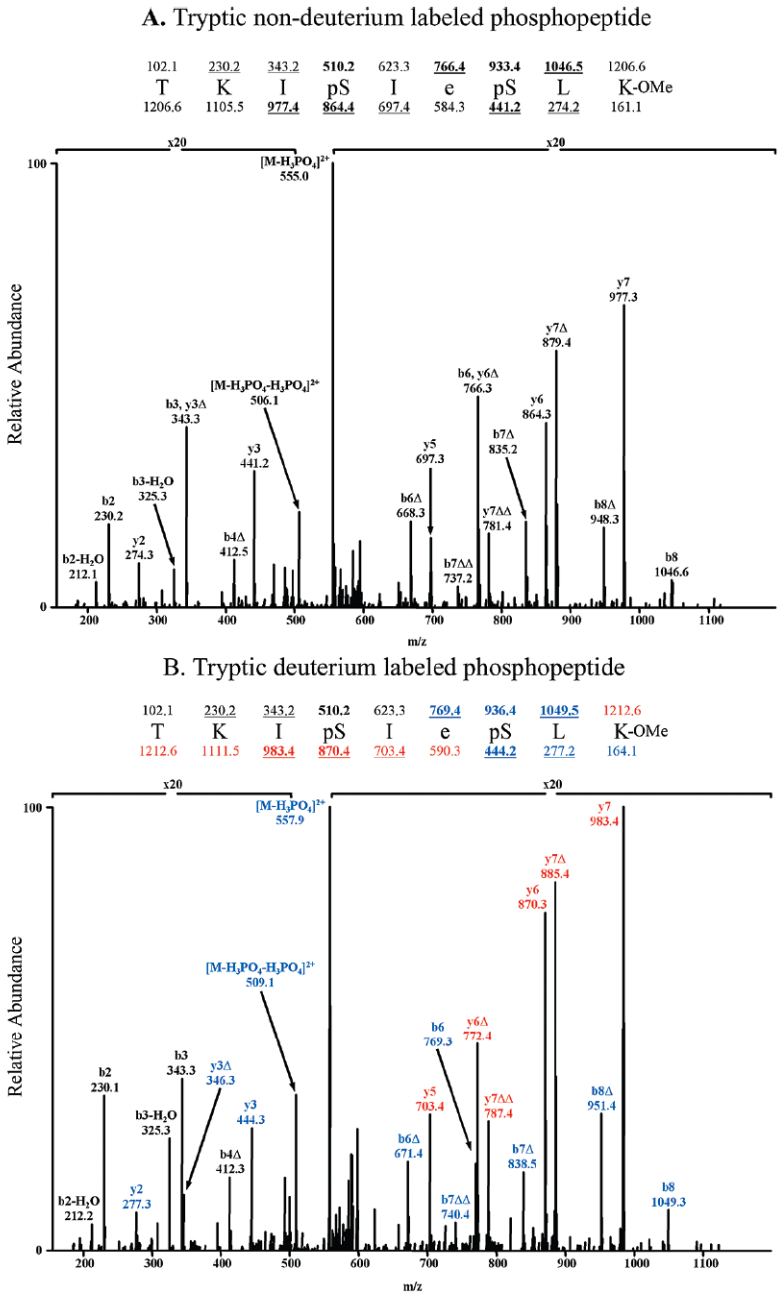


**Figure 4.**

MS/MS spectra of the tryptic deuterated (A) and nondeuterated (B) phosphopeptide TKIpSIepSLK. Predicted monoisotopic masses for the ions of type b and y are shown above and below the sequence, respectively. Ions observed in the spectrum are underlined and those that lose phosphoric acid are presented in bold type. The label, Δ, denotes loss of phosphoric acid from the corresponding ion of type b or y. K-OMe represents the Fisher esterified C-terminal lysine, while “e” represents the Fisher esterified glutamic acid. Masses for b and y ions which are shifted by +3 amu in the deuterated spectra are presented in blue, while those ions shifted by +6 amu are presented in red.

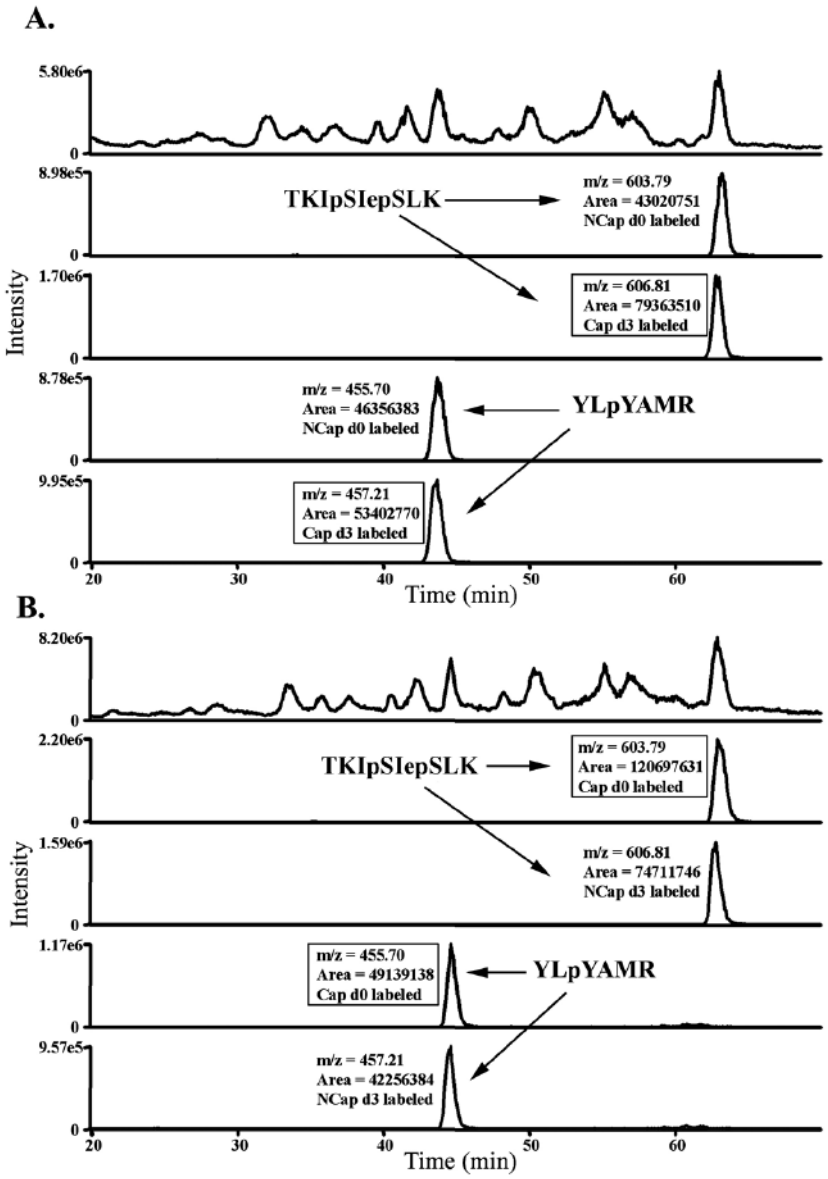


**Figure 5.**

Total ion chromatograms and single ion chromatograms for the differentially labeled tryptic phosphopeptides TKIpSIepSLK and YLpYAMR from the $d_0$ noncapacitated/$d_3$ capacitated analysis (A) and the $d_0$ capacitated/$d_3$ noncapacitated analysis (B). Note that the peak areas for the peptides from the capacitated sample are greater in each analysis, demonstrating that this phenomenon is sample specific and not an artifact of the differential labeling.

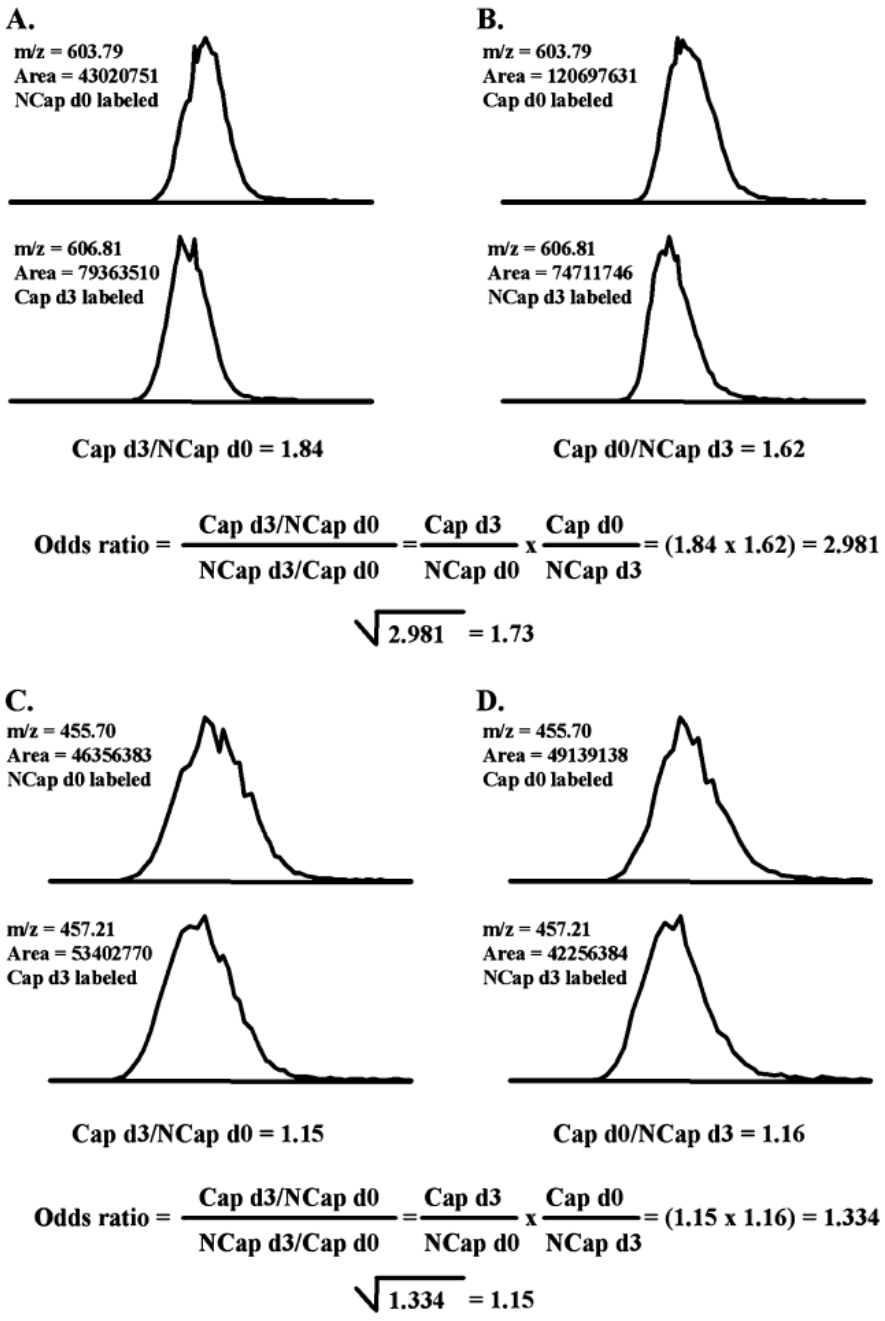


**Figure 6.**

Single ion chromatograms for the differentially labeled tryptic phosphopeptides TKIpSIepSLK and YLpYAMR from the $d_0$ noncapacitated/$d_3$ capacitated analysis (A and C, respectively) and the $d_0$ capacitated/$d_3$ noncapacitated analysis (B and D, respectively). The square root of the ratio of the $d_3/d_0$ ratios (odds ratio) for each peptide was calculated as indicated, in order to remove potential errors associated with the comparison of the deuterated and a nondeuterated peptide species.

**Table 1**

Phosphopeptides Identified in Capacitated (Cap) and Noncapacitated (NCap) Mouse Sperm Total Protein Digests, and Their Relative Quantitation Based upon the Square of the Odds Ratio (OR)[a]

| phosphopeptide sequence | charge | exp. *m/z* | calc. *m/z* | phosphosites | NCBI accession number | protein name | OR Cap/Ncap |
|---|---|---|---|---|---|---|---|
| K.NIdLTAIIpSdLR.S | 2 | 733.39 | 733.39 | 1 | AAH57001 | Outer Dense fiber 2 (Odf2) protein | Only in Ncap |
| K.AIVpSPPVeMVeeIpSK.D | 2 | 922.44 | 922.43 | 2 | XP_139384 | Recently removed from NCBI database | 0.04 |
| K.TSApTeIQSeLSSMR.Y | 3 | 554.58 | 554.59 | 1 | NP_080569 | Sperm acrosome associated 1 | 0.56 |
| K.(pTpS)ATeIQSeLSSMR.C | 2 | 831.38 | 831.38 | 1 | NP_080569 | Sperm acrosome associated 1 | 0.62 |
| K.(pTpS)ATeIQpSeLSpSMR.Y | 2 | 911.35 | 911.34 | 3 | NP_080569 | Sperm acrosome associated 1 | 0.74 |
| R.deMVAGpSQepSIK.V | 2 | 755.30 | 755.30 | 2 | NP_780347 | Dynein, axonemal, intermediate chain 1 | 0.74 |
| R.TLpSdYNIQK.E | 2 | 595.28 | 595.28 | 1 | CAI24672 | Ubiquitin B | 1.12 |
| K.YLpYAMR.L | 2 | 455.69 | 455.70 | 1 | AAB57760 | Hexokinase | 1.16 |
| R.TTpSMSHVGpSAIMVdLPR.T | 3 | 663.95 | 663.96 | 2 | XP_355541 | Hypothetical Protein LOC381580 | 1.27 |
| K.TLKPGPGAHpSPeK.V | 3 | 476.24 | 476.24 | 1 | NP_081295 | SHIPPO-1 | 1.34 |
| R.VPpSPR.R | 2 | 325.16 | 325.16 | 1 | BAC26111 | Unknown | 1.36 |
| R.LpSPdYK.R | 2 | 415.69 | 415.69 | 1 | BAB24132 | Unknown | 1.37 |
| K.eIeQpSPPGpSPK.A | 2 | 685.79 | 685.79 | 2 | AAK49990 | Calcium Binding Protein CBP86–6 | 1.39 |
| K.(pTpS)ATeIQpSeLpSpSMR.C | 2 | 951.33 | 951.33 | 4 | NP_080569 | Sperm acrosome associated 1 | 1.44 |
| K.(pTpS)AQVVVGPVSeAePPK.A | 2 | 908.97 | 908.96 | 1 | AAK49990 | Calcium Binding Protein CBP86–6 | 1.58 |
| K.SepSLQALQdK.V | 2 | 620.80 | 620.80 | 1 | AAH50799 | Spata18 protein | 1.60 |
| R.pSPSHpSPATSApSYIGPIR.N | 2 | 991.40 | 991.40 | 3 | EU937514 | Testis-specific serine/proline-rich protein[b] | 1.61 |
| R.SIpSQTGpSR.Q | 2 | 505.19 | 505.19 | 2 | NP_001074565 | Hypothetical Protein LOC75811 | 1.63 |
| K.pSMVLGYWdIR.G | 2 | 674.32 | 674.31 | 1 | NP_742035 | Glutathione-S-Transferase | 1.66 |
| K.TKIpSIepSLK.T | 2 | 603.79 | 603.79 | 2 | AAK49990 | Calcium Binding Protein CBP86–6 | 1.73 |
| R.pSPSHpSPATpSASYIGPIR.N | 2 | 991.40 | 991.40 | 3 | EU937514 | Testis-specific serine/proline-rich protein[b] | 1.77 |
| K.ApSLLpSNPIPeVK.T | 2 | 728.35 | 728.35 | 2 | CAB57454 | Testicular Haploid Expressed Gene (THEG) protein | 1.91 |
| K.SPpSQTGLK.N | 2 | 456.22 | 456.22 | 1 | CB273841 | McCarry Eddy round spermatid cDNA | 1.91 |
| R.SPpSHpSPATSApSYIGPIR.N | 2 | 991.40 | 991.40 | 3 | EU937514 | Testis-specific serine/proline-rich protein[b] | 1.96 |
| R.ASpSQpSPpSPHVQHVPR.G | 2 | 934.37 | 934.37 | 3 | EU937514 | Testis-specific serine/proline-rich protein[b] | 1.99 |
| R.ApSpSQpSPSPHVQHVPR.G | 2 | 934.37 | 934.37 | 3 | EU937514 | Testis-specific serine/proline-rich protein[b] | 1.99 |
| R.dLLpSIpSdGR.G | 2 | 589.25 | 589.25 | 2 | AAH27526 | Myeloid Leukemia Factor 1 (Mlf1) | 2.06 |

| phosphopeptide sequence | charge | exp. *m/z* | calc. *m/z* | phosphosites | NCBI accession number | protein name | OR Cap/Ncap |
|---|---|---|---|---|---|---|---|
| R.(pYpS)KepSLdAeK.R | 2 | 693.29 | 693.29 | 2 | AAK39109 | Autoimmune Infertility-related Protein | 2.09 |
| R.pSPSHpSPATSASYIGPIR.N | 2 | 951.42 | 951.41 | 2 | EU937514 | Testis-specific serine/proline-rich protein[b] | 2.19 |
| R.(pSpY)epSpSIdeNeGYQK.S | 2 | 979.85 | 979.84 | 3 | AAH06583 | Ccdc136 protein | 2.28 |
| K.GYpSVGdLLQeVMK.F | 2 | 780.88 | 780.87 | 1 | AAM18540 | A Kinase Anchoring Protein 4 (AKAP4) | 2.29 |
| R.SPpSHpSPATpSASYIGPIR.N | 2 | 991.40 | 991.40 | 3 | EU937514 | Testis-specific serine/proline-rich protein[b] | 2.49 |
| R.SPpSHpSPATSASYIGPIR.N | 2 | 951.41 | 951.41 | 2 | EU937514 | Testis-specific serine/proline-rich protein[b] | 3.13 |
| R.pSeGeLNLeTLeeK.E | 2 | 827.90 | 827.90 | 1 | AAM18540 | A Kinase Anchoring Protein 4 (AKAP4) | 3.27 |
| R.pSPpSHpSPATSASYIGPIR.N | 2 | 991.40 | 991.40 | 3 | EU937514 | Testis-specific serine/proline-rich protein[b] | 3.30 |
| R.KKpSPTpSAeLLLIdPR.Y | 2 | 935.49 | 935.48 | 2 | NP_083218 | Organic anion transporter, member 6c1 | 3.34 |
| R.SRpSPpSPIR.C | 2 | 537.23 | 537.23 | 2 | AAH50799 | Spata18 protein | 3.81 |
| K.IRpSPpSPNR.S | 2 | 550.74 | 550.74 | 2 | AAH50799 | Spata18 protein | 3.86 |
| R.ASpSQpSPSPHVQHVPR.G | 2 | 894.39 | 894.39 | 2 | EU937514 | Testis-specific serine/proline-rich protein[b] | 3.98 |
| K.TPTGQTHQpSPVSK.R | 2 | 731.86 | 731.34 | 1 | AAA40413 | Testis-specific protein | 4.01 |
| R.LSpSLVIQMAR.K | 2 | 606.31 | 606.32 | 1 | AAM18540 | A Kinase Anchoring Protein 4 (AKAP4) | 4.62 |
| K.KMpSpSMSLLFK.R | 2 | 673.29 | 673.29 | 2 | XP_573518 | Recently removed from NCBI database | 6.03 |
| R.RLTLPpSLSLQYdGAGR.S | 3 | 618.99 | 618.99 | 1 | EU937514 | Testis-specific serine/proline-rich protein[b] | 14.93 |
| K.LIpSSeNFeNYVR.E | 2 | 796.88 | 796.87 | 1 | AAH48437 | Fatty acid binding protein 9 (testis) | Only in Cap |

[a] Note that AIVpSPPVeMVeeIpSK is found to be downregulated by a factor of 25 in the capacitated sample, while LIpSSeNFeNYVR from fatty acid protein 9 is only detected in the capacitated sample. The peptide YLpYAMR from hexokinase is found at almost equal abundance in both samples, consistent with previously published reports, and serving as a control for this set of experiments. Esterified aspartic and glutamic acid residues are indicated by 'd' and 'e', respectively. Phosphoserine, phosphothreonine or phosphotyrosine residues are specified by pS, pT or PY, respectively. Phosphopeptides whose MS/MS spectra contain insufficient evidence to unequivocally assign the phosphate group to one of the N-terminal amino acids have both potential sites of phosphorylation shown in parentheses.

[b] Novel testis-specific serine/proline-rich protein. Salicioni et al., unpublished results.